Error negativity does not reflect Conflict. A re-appraisal of conflict monitoring and Anterior Cingulate Cortex activity [1]

3.1 Introduction

In order to adapt to ever-changing environments, animals must continuously alter their behavior. Such flexibility is often assumed to be mediated by "control" mechanisms that adjust information processing to the prevailing context. The way in which control mechanisms are recruited, however, remains obscure. In the last few years, the "conflict-loop theory" (Botvinick *et al.*, 2001, 2004, 1999; Carter *et al.*, 1999, 1998; Cohen *et al.*, 2000; Yeung *et al.*, 2004) has played an essential role in this field by providing a unified model that aims to account for both neurophysiological and behavioral aspects of control implementation. This model introduced a very simple, though very powerful, concept, namely "response conflict". Response conflict, measured by the Anterior Cingulate Cortex (ACC), is explicitly defined as the product of the activation of the responses weighted by the inhibitory connections between these responses (Botvinick *et al.*, 2001; Yeung *et al.*, 2004, see also eq. 3.2). In this type of neural network model, "response activation"

1. article publié dans la revue *Journal of Cognitive Neuroscience* 20 :9, pp. 1637–1655

refers to the amount of neural activity in the structures involved in response execution. Conflict monitoring has been largely studied in the so-called flanker task (Eriksen et Eriksen, 1974), in which participants must issue a right or a left hand response as a function of a target letter (*e.g.* the letters S or H), flanked by distractors that can be compatible (SSS) or incompatible (HSH) with the target. The implementation of the conflict model for the flanker task has been extensively described by Botvinick *et al.* (2001) and Yeung *et al.* (2004). Only the major aspects, and those directly relevant for our purpose, will be described here.

The model is implemented as a three–layers neural network (Cohen *et al.*, 1992) : one perceptual layer codes for the target and both distractors, one response layer codes for the two competing responses, and an attentional layer biases processing towards the target. All between–layer connections are excitatory (no between–layer inhibition), whereas all within–layer connections are inhibitory. To this basic architecture, the conflict modelers added a conflict–monitoring unit, that measures online the amount of conflict. Generally speaking, the conflict is measured as the energy (Hopfield, 1982) in the response layer, defined as :

$$-\sum\sum a_i a_j w_{ij} \tag{3.1}$$

where a represents the activity of each unit in the layer, indices $_i$ and $_j$ index the different units, and w_{ij} is the inhibitory connection between the units i and j.

In the flanker task, where only two possible responses are present, conflict over time, $Co(t)$, is computed as :

$$Co(t) = \begin{cases} -2 \times (act_H(t) \times act_S(t) \times -3) & if \quad act_H(t) > 0, act_S(t) > 0 \\ 0 & otherwise \end{cases} \tag{3.2}$$

where $act_H(t)$ - respectively $act_S(t)$ - is the activation level of the unit coding for the H response - respectively the S response - at time t, and -3 is the (constant) inhibitory connection between the left and the right response units.

Conflict monitoring is assumed to be measurable with fMRI (Barch *et al.*, 2000; Botvinick *et al.*, 1999; Carter *et al.*, 1998) and EEG (Gehring et Fencsik, 2001; Rodríguez-Fornells *et al.*, 2002; Van Veen et Carter, 2002; West, 2004; Yeung *et al.*, 2004). In the present study, we will concentrate on the EEG correlate : when participants commit an error, one observes a negative component, maximal fronto-centrally, called "Error Negativity" (N_e) (Falkenstein *et al.*, 1991), or "Error Related Negativity" (ERN) (Gehring *et al.*, 1993), starting about 30 ms and peaking about 100 ms after the incorrect electromyographic (EMG) activity. Simulations of the model have revealed that conflict is maximal just after the incorrect response activation ; its timing

is thus comparable to that of the N_E [2]. This similarity led Botvinick *et al.* (2001) and Yeung *et al.* (2004) to re-interpret the N_E in terms of conflict ; conflict that results secondarily in error detection. According to these authors, the time course of the N_E should parallel the time course of the conflict. One way of testing this view is to estimate conflict on a trial–by–trial basis. Since conflict is defined as the degree of co-activation of the responses, it amounts to estimating the degree of overlap between correct and incorrect response activations. One major difficulty is that response activation is a covert process, not directly observable. However, EMG recordings of the muscles involved in responding have proved efficient in revealing such covert activation (*e.g.* Burle *et al.*, 2005, 2002b; Coles *et al.*, 1985; Hasbroucq *et al.*, 1999; Smid *et al.*, 1990) : on some trials, although the correct response was given, subthreshold EMG activity in the muscles involved in the incorrect response ("partial error", see Figure 3.1A) can be observed. A N_E has been reported to occur just after such partial errors (Burle *et al.*, 2005; Masaki et Segalowitz, 2004; Vidal *et al.*, 2000). Since these partial errors are detectable on a trial–by–trial basis, they offer the unique opportunity to directly evaluate the activation of incorrect responses, not otherwise observable on overt performance. [3]

Importantly, conflict is defined as the degree of *co-activation* of the two responses (see eq. 3.2). We thus reasoned that it should depend on the temporal overlap between incorrect and correct response activations, that is on the time separating the incorrect from the correct response (Δ value on fig. 3.1). In order to verify the validity of this reasoning, we first ran a simulation study in which trials containing the equivalent of partial errors were analyzed. Since, as the results will show, this assumption was supported, the Δ value was the main variable of interest. We then compared the simulated data to real, experimental data (see below). In order to compare the simulation results with the experimental ones, we processed the simulation and the EEG data in the same way. To

2. According to the conflict model, conflict is maximal after the incorrect response on erroneous trials, but peaks just before the correct response on correct trials (see (Yeung *et al.*, 2004, Figure 14)). This is due to the fact that, on correct trials, the incorrect activation precedes the correct activation. It has been argued that, in this case, the electrophysiological correlates of the conflict is to be found on a "N2" component, either time–locked to the stimulus (Yeung *et al.*, 2004, Figure 15), or response-locked (Yeung *et al.*, 2004, Figure 13). As the simulations presented below will clearly show, this N2 in fact reflects a N_E time–locked to the incorrect response activation, as predicted by the conflict model.

3. Note that, although EMG-fMRI co-registration is now starting to become feasible, detecting such small incorrect EMG activations during fMRI acquisition is still beyond the current technical capabilities, since those partial errors are of small amplitude, and the frequency components of EMG largely overlaps the frequencies of the noise induced by the EPI. It is therefore currently technically impossible to measure the degree of response co-activation in the scanner. For this reason, EEG is more appropriate than fMRI to test this aspect of the model.

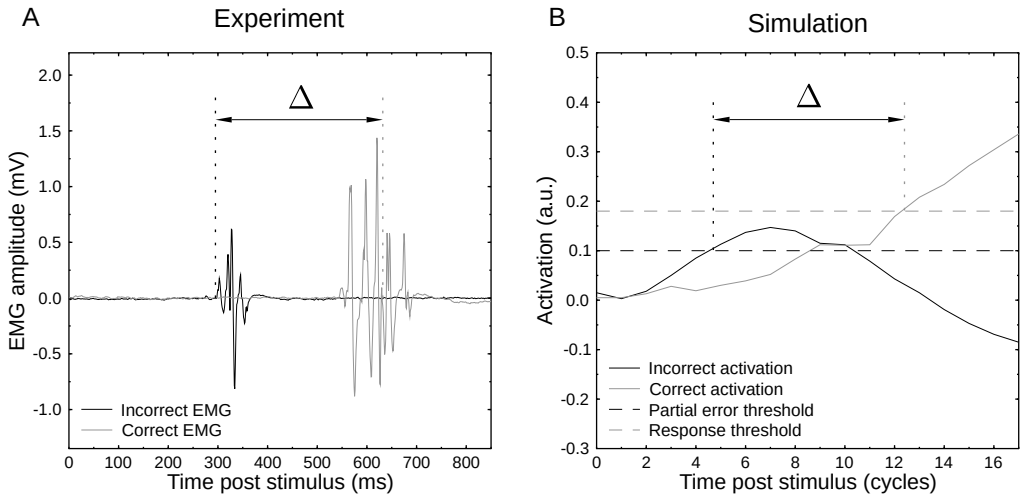

FIGURE 3.1 – Examples of "partial errors" obtained in the experiment and in the simulation. (A) The left part of the graph presents the electromyographic (EMG) activity as a function of time, in the muscles involved in the execution of the incorrect (black) and in the correct responses (grey). The time origin corresponds to stimulus presentation. The vertical black dashed line corresponds to the onset of the partial error, and the vertical grey dashed line to the mechanical response. Although the correct response was given, one can observe an activation of the incorrect response whose amplitude is, however, too low to trigger an overt error. The time interval between the incorrect EMG onset and the correct mechanical response is defined as Δ, and will be used as an index of the temporal overlap between the two response activations. (B) The right part of the figure presents a simulated trial, with the amount of activation (in arbitrary units) of the incorrect (black line) and of the correct (grey line) response as a function of time. The time–zero corresponds to stimulus presentation, the vertical black dashed line corresponds to the onset of the partial error, and the vertical grey dashed line to the timing of the response. The two horizontal long dashed lines correspond to the partial error threshold (black) and to the correct response threshold (grey)

this end, we used the open-source software EEGLAB (Delorme et Makeig, 2004) which allows single-trial dynamics to be studied Jung *et al.* (2001) and hence reveals more precisely the impact of Δ value on conflict and N_E amplitudes.

3.2 Methods

3.2.1 Simulation study

Simulation parameters

The simulation was based on 10 runs (representing 10 participants) of 1,000 trials each. All parameters used in the simulation were those used previously in the studies of Botvinick *et al.* (2001) and Yeung *et al.* (2004) [4], except the threshold for "partial errors" (which were not previously considered). In the previous simulations, a response was recorded as soon as one of the two response units reached an activation level of .18. Using this value, a pilot simulation study indicated that a threshold of .10 for partial errors gives 10-15% partial errors, which is equivalent to the percentage usually obtained in empirical studies (Burle *et al.*, 2002b; Gratton *et al.*, 1988; Hasbroucq *et al.*, 1999; Smid *et al.*, 1990). Importantly, changing this value modified the overall number of partial errors, but did not affect the global performance pattern, as the difference in partial errors rate between compatible and incompatible trials remained constant whatever this value (though within realistic limits). Thus the results presented below are not specific to a well–tuned, somewhat arbitrary, value that we have chosen for partial errors threshold.

Data preprocessing

Depending on whether the correct or incorrect response unit reached the response threshold first, the trial was classified as correct or erroneous, respectively. Among the correct trials, we checked whether the incorrect response unit reached the partial error threshold before the correct response (it never happened that the incorrect response layer reached the partial error threshold *after* the correct response). If the incorrect unit reached the predefined threshold of .10, the trial was classified as a partial error trial. In order to have enough trials available for analysis in both the simulation and the experiment, we focused on incompatible trials containing partial errors, since the number of partial errors is higher in incompatible situations (Burle *et al.*, 2002b; Coles

4. Botvinick *et al.* (2001) implemented two versions of the model : one with a feedback on the attentional layer, one without. The version used here implements the feedback.

et al., 1985; Gratton *et al.*, 1988; Smid *et al.*, 1990).

The individual partial error trials were thereafter imported into EEGLAB (Delorme et Makeig, 2004) for further analysis (see "Single trial analysis" section).

3.2.2 Experimental study

Participants

Ten right-handed participants (3 women, 7 men, aged from 20 to 31 years, mean age = 25 years) volunteered for this experiment. They all had normal or corrected-to-normal vision. Before the study, all the participants gave their informed written consent according to the Declaration of Helsinki. They were informed of the purpose and procedure of the experiment before participating.

Experimental task and procedure

The participants performed an Eriksen's flanker task (Eriksen et Eriksen, 1974) in which they had to respond with a right or a left thumb keypress as fast as possible as a function of a central target letter (S or H) flanked by two distractors that could be compatible (*e.g.* SSS) or incompatible (*e.g.* HSH). The stimuli were presented by a seven–segments light-emitting-diodes display (Lextronic, model SGN-S5, 33 × 14 mm), located 1.5 m in front of the participant. The stimuli were extinguished with the participants' response. The participants held vertical hand-grips on top of which response buttons were fixed.

Participants performed 20 blocks of 128 trials each. After stimulus presentation, they had 1 s to respond. The next stimulus was delivered 1 s after the response. All types of trials (HHH, HSH, SHS and SSS) were equiprobable and presented in a pseudo-random order.

Data acquisition and preprocessing

Electroencephalographic (EEG) and electromyographic (EMG) activity was recorded with Ag/AgCl electrodes (BIOSEMI Active-Two electrodes, Amsterdam). The sampling rate was 1024 Hz (filters : DC to 268 Hz, 3 dB/octave). For EEG, we used 64 channels (10-20 system positions). The vertical EOG was recorded by means of two electrodes (same type as EEG) just above and below the left eye, respectively, and the horizontal EOG was recorded with two electrodes positioned over the two outer canthi. EMG was recorded by means of two pairs of electrodes glued to the skin of the thenar eminence above the *flexor pollicis brevis* of each hand. The distance between the two EMG electrodes was 2 cm.

After acquisition, the electrophysiological data were filtered (EEG : high-pass = 0.3 Hz, low-pass = 100 Hz and EMG : high-pass = 10 Hz). Eye movement artifacts were corrected by the statistical method of Gratton *et al.* (1983). All other artifacts were rejected after visual inspection of individual traces. The onset of the EMG activity was marked manually after visual inspection. Indeed, although automated algorithms can be useful, visual inspection remains the most accurate technique against which all algorithms are compared (Staude *et al.*, 2001; Van Boxtel *et al.*, 1993), especially for detecting small changes in EMG activity such as partial errors. Importantly, the experimenters were not aware of the nature of the trial (compatible *vs* incompatible) being processed. Furthermore, the EEG signals corresponding to the current EMG were not displayed when detecting EMG onset. Thus, the experimenter was completely blind regarding all the other relevant parameters, and hence could not, even unwittingly, bias the results.

The trials were classified as correct or erroneous, depending on whether the correct or the incorrect button was pressed first. Among the correct trials, we separated trials containing only one EMG activation on the correct side, from trials containing an EMG activation on the incorrect side preceding the correct response (partial error trials, see Figure 3.1A). Laplacian transformation, as implemented in BrainAnalyser© (Brain Products, Munich), was applied to each individual trial to increase the spatial resolution of the EEG (Babiloni *et al.*, 2001) : first the signal was interpolated with the spherical spline interpolation procedure (Perrin *et al.*, 1989), and hence the second derivatives in two dimensions of space were computed. We choose 3 for the degree of spline since this value minimizes errors (Perrin *et al.*, 1987), and the interpolation was computed with a maximum of 15 degrees for the Legendre polynomial. We assumed a radius of 10 cm for the sphere representing the head, rather than the unrealistic default radius of 1 m assumed by BrainAnalyser©. With such a realistic radius, the most suitable unit is $\mu V/cm^2$. The individual Laplacian transformed trials were imported in EEGLAB for further analysis.

3.2.3 Temporal overlap estimation

In order to compare temporal overlap in simulated and experimental data, we choose a functionally equivalent measure for both. This measure, the Δ value depicted on Figure 3.1, corresponds to the time between the onset of the partial error and the moment of the correct response (Figure 3.1A) for the experimental data, and to the "time" (represented in "cycles") between the partial error threshold (.10) and the correct response one (.18, Figure 3.1B) for the simulations. In both cases, a greater Δ value indicates a longer time between the incorrect response activation and the

correct response, revealing a lower temporal overlap. In the following we will use the Δ value as a measure of temporal overlap.

3.2.4 Single trial analysis

EEG signal analysis normally relies on averaging techniques. Averaging, however, induces a considerable loss in the dynamics of the process of interest (Jung *et al.*, 2001), as will also be exemplified below. We therefore resorted to the "ERP-image" technique, implemented in the EEGLAB software (Delorme et Makeig, 2004), allowing one to visualize brain activity without averaging. This technique has been detailed elsewhere (Jung *et al.*, 2001), and will only be briefly described here. Note that this technique was applied not only to the Laplacian-transformed EEG data, but also to the simulated data. To construct the individual ERP-images, the trials are first sorted based on a relevant measure. In our case, for both the simulation and the experimental data, the time–zero corresponds to the onset of the partial error, and the trials are arranged by increasing Δ values. The trials are then plotted as parallel colored lines. The result is a "raster–like" plot, with the x-axis representing time, the y-axis representing the arranged trials, and a color code indicating the intensity of the signal for each trial and each time point. On all figures, the vertical black line indicates the onset of the partial error, and the S-shaped one indicates the correct response. Below each raster–like plot, the average of the traces are represented as a function of time, hence giving an estimate of the activity under analysis. For the simulation, the blue color indicates conflict (positive values), whereas for the experimental data, blue represents negative polarity. This was done to improve the comparability between the conflict and the N_E, both appearing in blue in the ERP–images.

ERP-images have been computed for each participants : for the experimental data, the ERP–images are based on the individual Laplacian–transformed trials. For the simulation, this was performed on the individual activation function and/or the computed conflict traces. Besides individual subject representations, we sought for a population–based representation of the data. One way of doing so, is to put all the trials of all the subjects in the same ERP-Image. This approach has some strengths and limitations. The main interest is that one can visualize all trials of all subjects. However, the within–subject variance, in amplitude and in Δ values, is confounded with the between–subject variance : for example, subjects with short Δ values will mainly contribute to the lower part of the ERP-Image, whereas subjects with long Δ values will mainly be present on the upper part. A similar bias holds for amplitude. Finally, data represented in this way are

not comparable to more traditional grand-averaged representation. One alternative approach is to built a "grand averaged" ERP–image by averaging the individual ERP-Images (see Appendix A for further details). In this case, all subjects have the same weight at every points of the ERP-Image, allowing one to visualize the impact of Δ values on the population without bias induced by between-subject variability. One disadvantage, however, is that we do not see in this case "real" individual trials, but averaged ones for a given normalized Δ value. Since these two methods have complementary strengths and shortcomings, we present the two representations along with individual ERP-Images. Since these various approaches led to very consistent results, despite their different strengths and drawbacks, we considered that the features expressed on these analyses could not be artifacts induced by any of the methods.

As recommended by Jung *et al.* (2001) the ERP–images have been smoothed, with a smoothing width set at about 10% of the number of trials. One exception, however, is to be noted for the primary motor cortices activations (Figure 3.7C and D) : since the activities of interest were of small amplitude leading to a lower signal/noise ratio, the smoothing step was set at about 20%.

Statistical analysis

ERP–images, although very informative, do not allow one to statistically validate the observed features. To do so, both the simulated and experimental trials were binned into different classes depending on the Δ interval. The classes were of equal width.

For the simulation, four classes of 3 cycles were retained that contained the largest number of trials for a reliable estimate of the conflict amplitude : class 1 = from 2 to 4 cycles, class 2 = from 5 to 7 cycles, class 3 = from 8 to 10 cycles and class 4 = from 11 to 13 cycles. The conflict signals obtained on each trial were then averaged, time–locked to the partial error onset for each class, and each run separately. The peak of conflict was determined as the maximum value in a window starting from the partial error onset and lasting 20 simulation cycles. We measured the peak and latency of this peak. Besides these "static" parameters, we investigated the dynamic aspects of conflict by studying how conflict develops. To do so, we analyzed the rising slope of the conflict by fitting a linear regression to the conflict signal in a window from the partial error onset to the 4^{th} cycle following the partial error onset.

For the EEG data, the same method was applied : individual trials were binned as a function of the time separating the incorrect EMG onset from the correct response. Four classes that contained the larger number of trials (class 1 : from 101 to 150 ms, class 2 : from 151 to 200 ms, class 3 : from 201 to 250 and class 4 : from 251 to 300 ms) were retained. The EEG activity was averaged

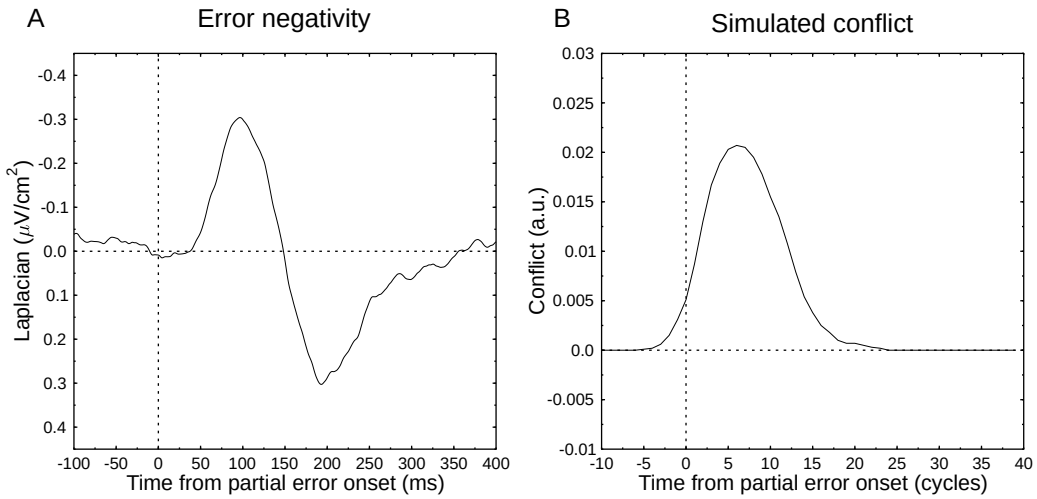

FIGURE 3.2 – **Comparison between grand–averaged N_E and conflict.**(A) Amplitude of the Laplacian transformed N_E induced by partial errors as a function of time. The time–zero corresponds to the partial error onset. A clear N_E can be observed starting about 30 ms after incorrect EMG onset and peaking about 100 ms after it. Furthermore, its topography is well localized fronto-centrally (see Figure 3.8 for the topography of this wave). (B) grand-averaged conflict as a function of time. Time–zero corresponds to crossing of the partial error threshold. The conflict is clearly maximal just after the partial error, and its timing nicely fits that of the N_E. This confirms that the N_E on partial errors is a valid measure for testing the conflict model predictions.

for each participant and for each class separately. As for the simulation, the parameter used to estimate the N_E was the amplitude of the peak of the N_E (defined as the difference between the positive peak occurring just after the partial error – between 10 and 50 ms – and the following negative peak – between 50 and 150 ms). We also analyzed how the N_E develops in time, by fitting a linear regression on the rising slope in a time window from 50 to 100 ms.

The statistical analysis involved either Student t tests, for comparisons between two means, or ANOVAs, for comparisons of more than two means. When ANOVAs were performed, the error term was always the interaction between the factor "participants" and the factor under analysis. Percentages and rates can not be tested directly with parametric methods, since their mean and variances are closely related. However, the arcsine transform ($p' = asin\sqrt{p}$, with p being the rate under analysis) has proved to be efficient in stabilizing the variances (Winer, 1971), and was therefore used consistently for each analysis involving rates.

3.3 Results

3.3.1 Behavioral data

The overall percentage of errors was 5.2%. The number of overt errors was higher in the incompatible condition (7.5%) than in the compatible one (2.9%), $t_9 = 6.55; p < .001$. For correct trials, reaction time was longer when the flankers were incompatible (416 ms) than when they were compatible (386 ms), $t_9 = 15.36; p < .001$.

The number of partial error trials (see Figure 3.1) was higher in the incompatible situation (21.7%) than in the compatible one (14.3%), $t_9 = 5.78; p < .001$, in line with previously reported empirical data (Burle *et al.*, 2002b; Coles *et al.*, 1985; Smid *et al.*, 1990) (more behavioral data, and a deeper comparison between the experimental and the simulated results on these issues are presented in Appendix B).

3.3.2 Comparison between conflict and N_E timing as a function of Δ

In previous simulation studies (Botvinick *et al.*, 2001; Yeung *et al.*, 2004), conflict was analyzed time–locked to the stimulus and/or to the response. Since here we introduce partial errors to the simulation, we first verified that a peak of conflict was indeed obtained just after the partial error. Figure 3.2A presents the grand-averaged N_E time-locked to partial error onset. As already reported (Allain *et al.*, 2004a; Burle *et al.*, 2005; Masaki et Segalowitz, 2004; Vidal *et al.*, 2000), a clear N_E was apparent just after partial errors. Furthermore, the N_E observed after partial errors is clearly localized fronto-centrally (see Figure 3.8). Figure 3.2B shows the grand–averaged conflict obtained in the simulations when time-locked to the partial error. As anticipated, the conflict is maximal just after the partial error, validating the comparison between N_E and conflict on partial error trials.

Figure 3.3 show the single trial dynamics of the N_E and of conflict. Panels A and C present the grand–averaged ERP–Images, whereas panels B and D present all trials of all subjects plotted together. Pannels E, F and G present single subject ERP-Images (see above for a presentation of these different approaches). Time–zero corresponds to the partial error onset in all cases, and the S–shaped black line indicates the occurrence of the correct response. One striking feature that appears in the comparison of the two graphs, is the difference in timing of the conflict and the N_E : although the simulated conflict shows an S–shape very similar to the correct response one, the N_E seems better time-locked to the partial error onset. It seems, however, that the width of

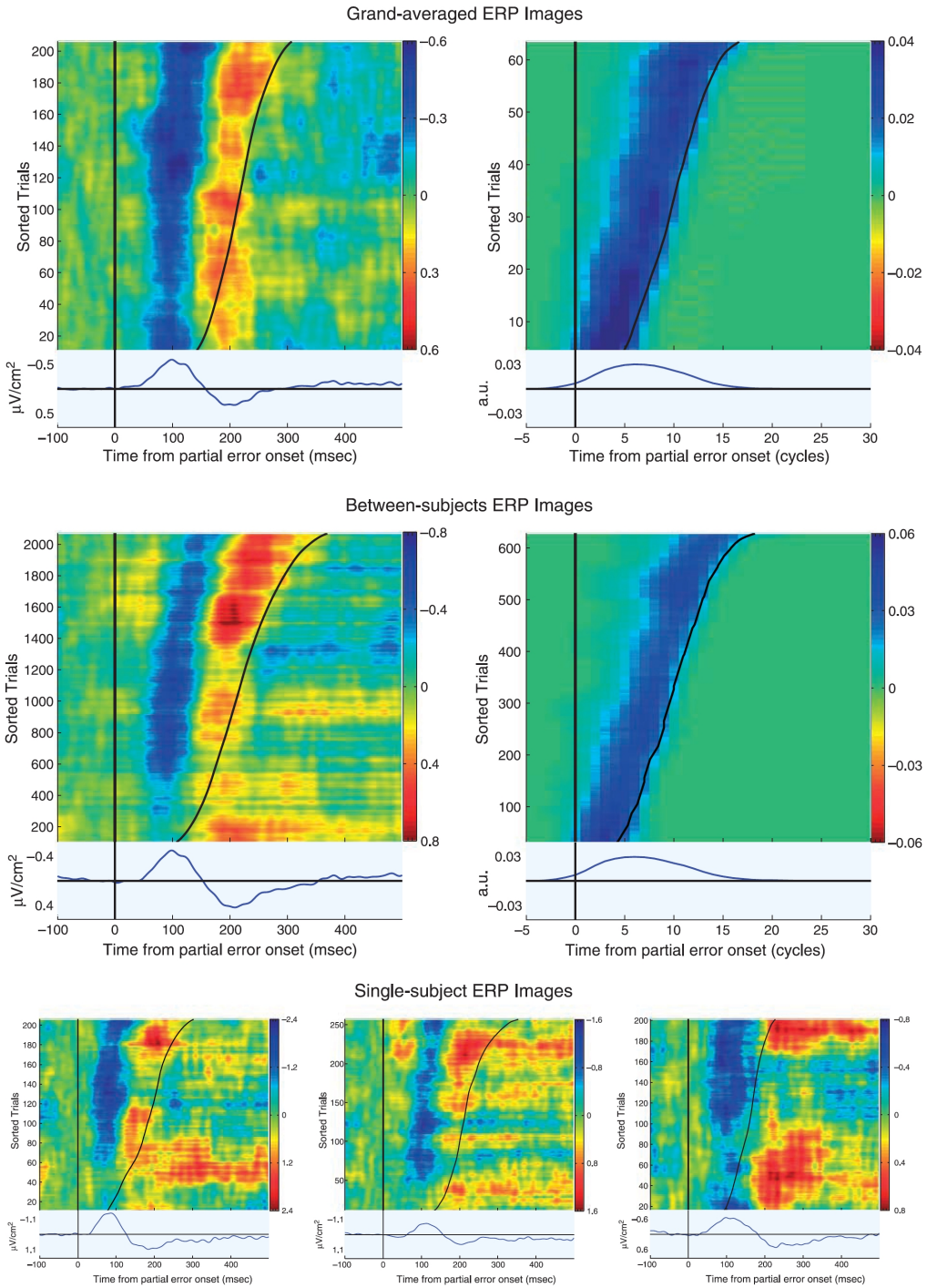

FIGURE 3.3 – **ERP-Images of the N_E and of the simulated conflict.** The trials containing a partial error were sorted as a function of increasing Δ values. The vertical black line indicates the onset of the partial error and the S-shaped black line indicates the moment of the correct response. (A and B) Grand-Average ERP-Images of N_E and simulated conflict. (C and D) Grand ERP-Image, containing all trials of all "subjects" for the N_E and the simulated conflict, respectively. (E,F and G) examples of individual ERP-Images. Whatever the representation, the conflict appears more time-locked to the correct response, contrary to the N_E, which appears more time-locked to the incorrect response activation.

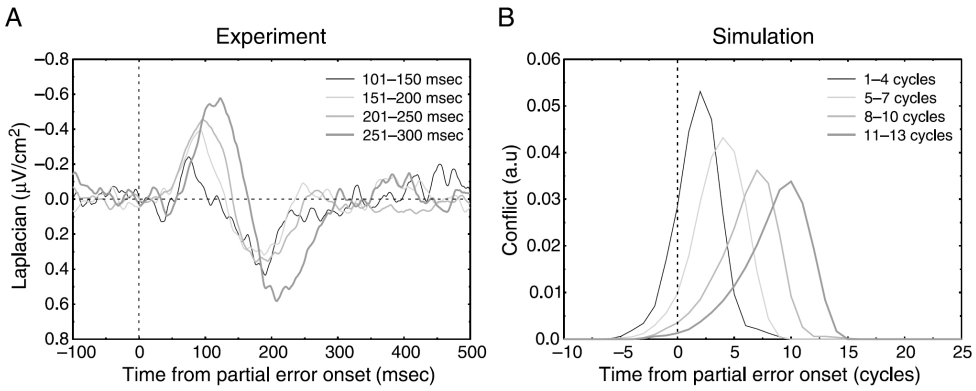

FIGURE 3.4 – (A) Classes analysis : Amplitude of the N_E (30 Hz low-pass filtered) as a function of time, for the four classes retained. Time zero corresponds to the onset of the partial error (see Figure 3.1). The amplitude of the N_E increases as Δ increases. (B) Amount of conflict as a function of time, for the four classes retained. Time zero corresponds to the moment at which the partial error threshold (.10) was crossed. The amplitude of the conflict, measured at the peak, decreases as Δ increases, therefore invalidating the proposition that the N_E reflects conflict.

the N_E increases as Δ increases. To clarify these points, we binned the trials into different classes varying in term of Δ (see the "Methods" section).

The grand average EEG data for each class is presented on Figure 3.4A. An ANOVA conducted on the peak amplitude revealed an effect of Δ, $F(3, 27) = 3.91, p < .05$: the smaller the Δ, the smaller the N_E. The latency of the peak was also affected by Δ, $F(3, 27) = 7.42, p < .001$, with the peak occurring earlier for small Δ than for large Δ. In contrast, no effect of Δ was observed on the rising slope of the N_E, $F(3, 27) = 1.34, p = .28$. Therefore, the latency effect is simply a consequence of the fact that, with the rising slope being the same but the amplitude higher, the peak is reached later.

The same analysis was performed on conflict (Figure 3.4B). ANOVAs revealed a clear effect of Δ on the amplitude of conflict, $F(3, 27) = 400.24, p < .001$: the smaller the Δ, the higher the peak of conflict. The latency of the peak of conflict was also affected by Δ, $F(3, 27) = 409.17, p < .001$, with a peak of conflict occurring later as Δ increased. Finally, the rising slope of the conflict was also steeper when Δ was low than when it was high, $F(3, 27) = 20.72, p < .001$. It therefore appears that the amplitude of conflict decreases as Δ increases. The dynamics of the conflict are also affected, since the rising slope is sensitive to Δ.

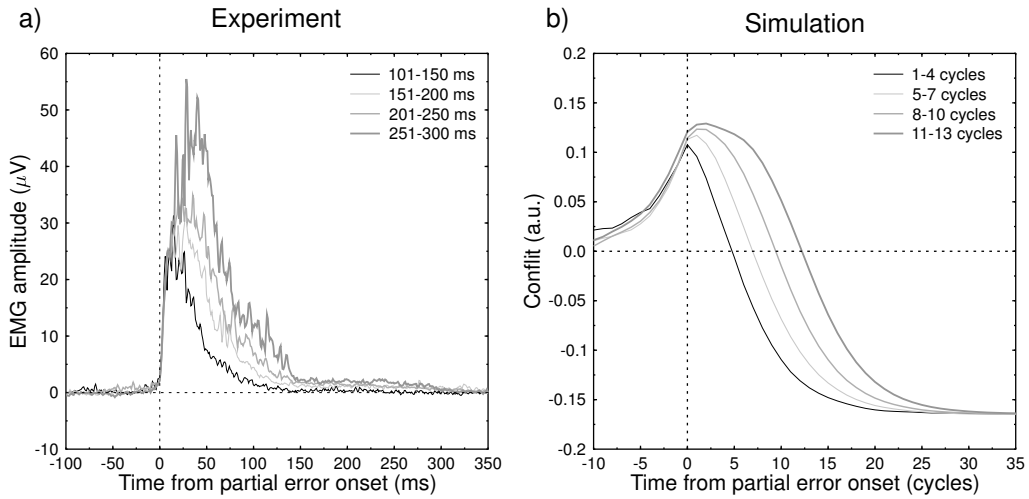

FIGURE 3.5 – **Amount of incorrect response activation as a function of Δ.** (A) Grand averaged full-wave rectified EMG for the four classes retained. The amount of EMG increases as Δ increases. (B) Grand average of incorrect response activation in the simulation, for the four classes. As for EMG, the amount of incorrect response activation increases as Δ increases. The horizontal line at .10 indicates the threshold for a partial error.

Alternative measure of conflict

Although the sensitivity of the N_E to Δ is opposite to that of conflict as defined in the model, conflict seems to last longer when Δ increases. We therefore evaluated whether a slight modification of the conflict computation could account for the data : instead of assuming that conflict at time t is the degree of co-activation of the two responses at time t, let's consider that it reflects the integration of such co-activation over time, that is conflict at time t could be :

$$Co(t) = \sum_{0}^{t} -2 \times (act_H(t) \times act_S(t) \times -3) \tag{3.3}$$

As a matter of fact, this quantity is assumed to be used for sequential adjustments (Botvinick *et al.*, 2001, see however Burle *et al.*, 2005). We therefore estimated the surface under the conflict curve for each simulated participant and for each class. This analysis revealed no change in conflict as a function of class ($F < 1$). Therefore, even the integrated conflict does not increase as Δ decreases, contrary to the N_E.

3.3.3 Conflict and the dynamics of incorrect and correct response activation

The above presented results are in clear disagreement with the interpretation of the N_E in terms of conflict. More specifically, the amplitude of the N_E does not parallel the degree of conflict. To better understand where the discrepancy comes from, we studied in more detail the activation dynamics of the incorrect and correct responses.

Conflict and the amount of incorrect response activation

When referring to eq. 3.2, it appears that conflict does not only depend on the temporal overlap between the two responses, but also on the amount of incorrect response activation (see simulation 5 of Yeung *et al.*, 2004). Differences in incorrect response activations might explain the observed discrepancy. To evaluate this, we averaged the simulated activation function of the incorrect responses, time-locked to the partial error onset for the four classes retained above. We processed the experimental data in a similar way : we took the size of the partial error EMG burst as an index of the incorrect response activation. To do so, the EMG bursts were rectified and then averaged separately for the same four classes used for the N_E. Figure 3.5 presents the results of this analysis. As one can see, for both the experimental (Figure 3.5A) and simulated (Figure 3.5B) data, the amount of incorrect response activation was greater when Δ was high. Indeed, the size of the partial error (*i.e.* the amount of EMG) increased as the interval between the incorrect and correct response activation got larger, $F(3, 27) = 24.43, p < .001$. The linear component was also significant, $F(1, 9) = 46.67, p < .001$. The simulation results were similar : the amount of incorrect response activation increases as Δ increases, $F(3, 27) = 71.45, p < .001$; linear component : $F(1, 9) = 160.1, p < .001$. These results have two important consequences. The first one is that, as anticipated, conflict is more sensitive to temporal overlap than to the mere amount of incorrect response activation. Indeed, the maximum conflict was obtained in the situation where the activation of the incorrect response was the lowest. Second, since the same increase in incorrect response activation is observed in the experimental and simulated data, the difference between the N_E amplitude and conflict cannot be explained by a difference in response activation.

Dynamics of correct and incorrect responses activations

We further explored the discrepancy between conflict and the N_E, by investigating the "empirical conflict" present in the experimental data, that is the degree of co-activation of the alternative

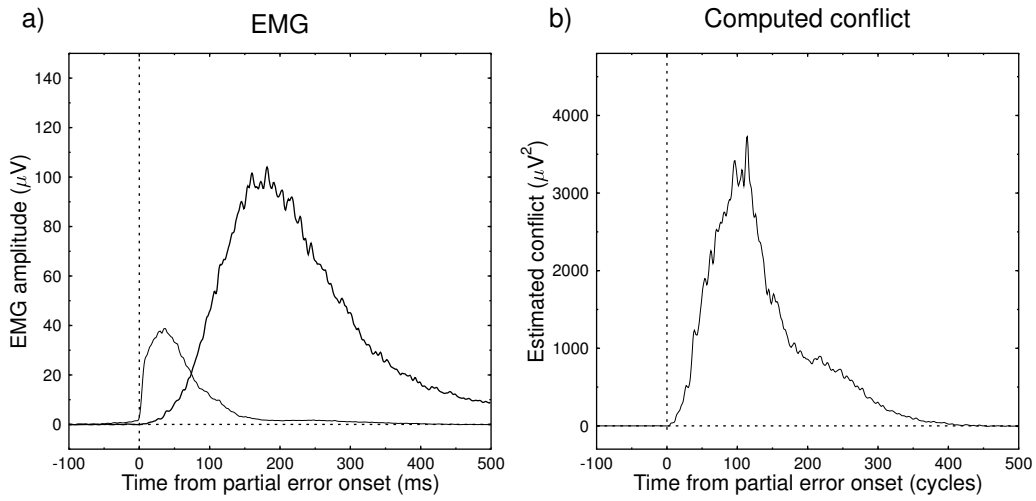

FIGURE 3.6 – **Empirical co-activation and conflict measured on the averaged traces.** (A) Temporal overlap of incorrect and correct response activation as measured with averaged EMG. The two responses appear to be co-activated around 100 ms after partial error onset. (B) empirical conflict obtained by applying eq. 3.2 to the averaged EMG activities. The empirical conflict nicely fits the prediction of the model, with conflict occurring shortly after the incorrect response activation, and peaking around 100 ms. This similarity, however, is an artifact due to averaging.

responses. We first analyzed the dynamics of response activation as estimated at the EMG level. Indeed, EMG seems a consensual measure of response activation, since, according to Yeung *et al.* (2004, p. 937) "Gehring et Fencsik (1999) have reported [...] that the ERN coincides with periods of co-activation of the correct and incorrect responses as measured through electromyography (EMG)". A similar argument was also put forward by Botvinick *et al.* (2001, p. 635). To evaluate the "empirical conflict" we applied eq. 3.2 to the averaged EMG traces, time-locked to the incorrect EMG onset (Figure 3.6A).

The two *averaged* EMG activities overlap around 100 ms after partial error onset, which replicates previous results (Gehring et Fencsik, 1999; Masaki et Segalowitz, 2004). Figure 3.6B presents the estimated conflict, after applying eq. 3.2 to these *averaged* EMG data. The estimated "conflict" starts just after the partial error onset, and peaks about 100 ms after it. This timing almost perfectly fits the one of the N_E reported on Figure 3.2A. This replicates the data of Gehring et Fencsik (1999). This apparent similarity is, however, an averaging artifact (Callaway *et al.*, 1984), as demonstrated below.

The first row of Figure 3.7 presents the ERP-images for the incorrect (panel A) and correct (panel B) EMG. A striking effect emerges from these ERP-images : although the duration of the

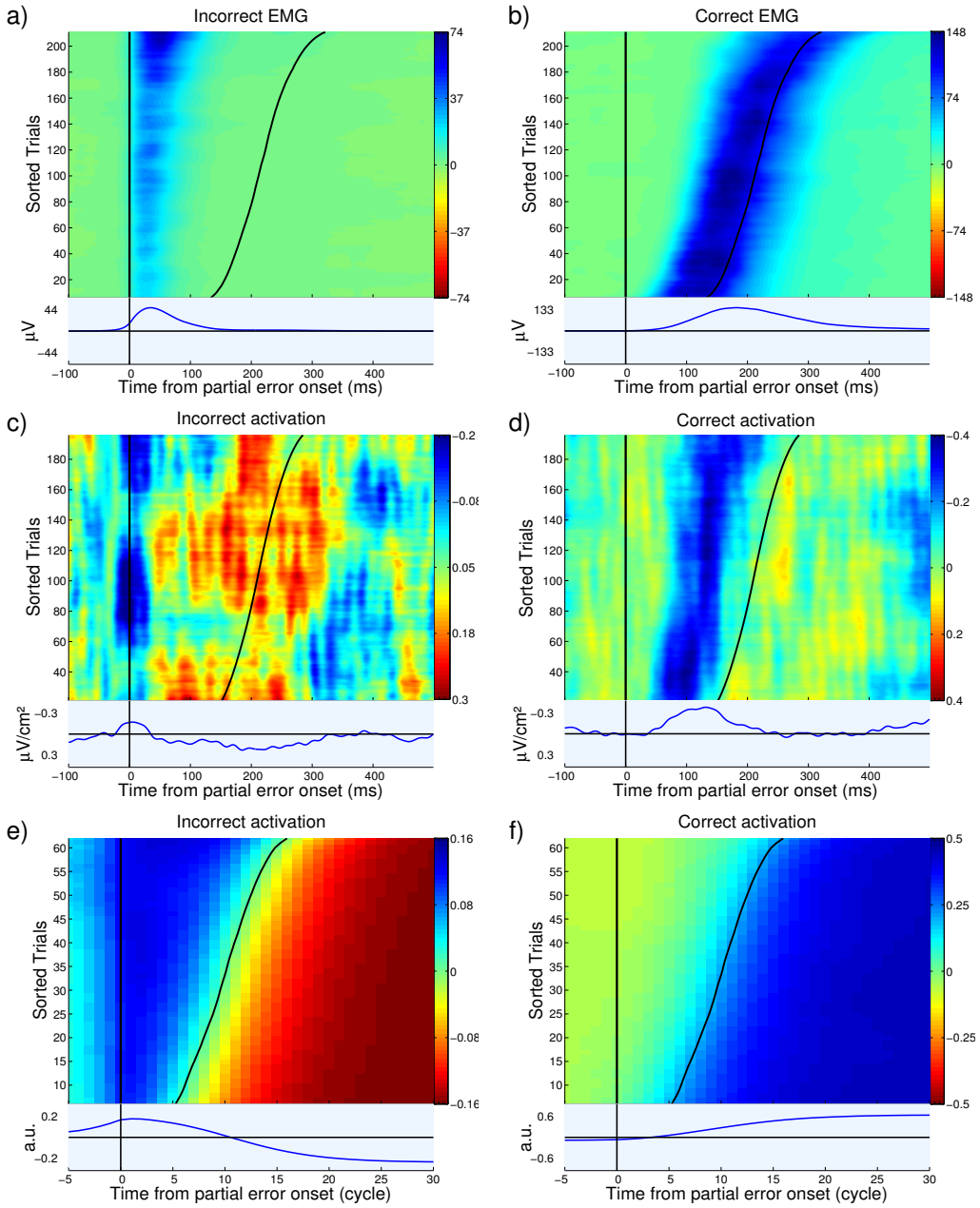

FIGURE 3.7 – **Single trial analysis of response activation.** This figure presents the incorrect (left column) and the correct (right column) response activations as a function of Δ, for the experiment as estimated by EMG amplitude (first row), or at the cortical level through the Laplacian estimated over the primary motor cortices (second row), and for the simulation (third row)

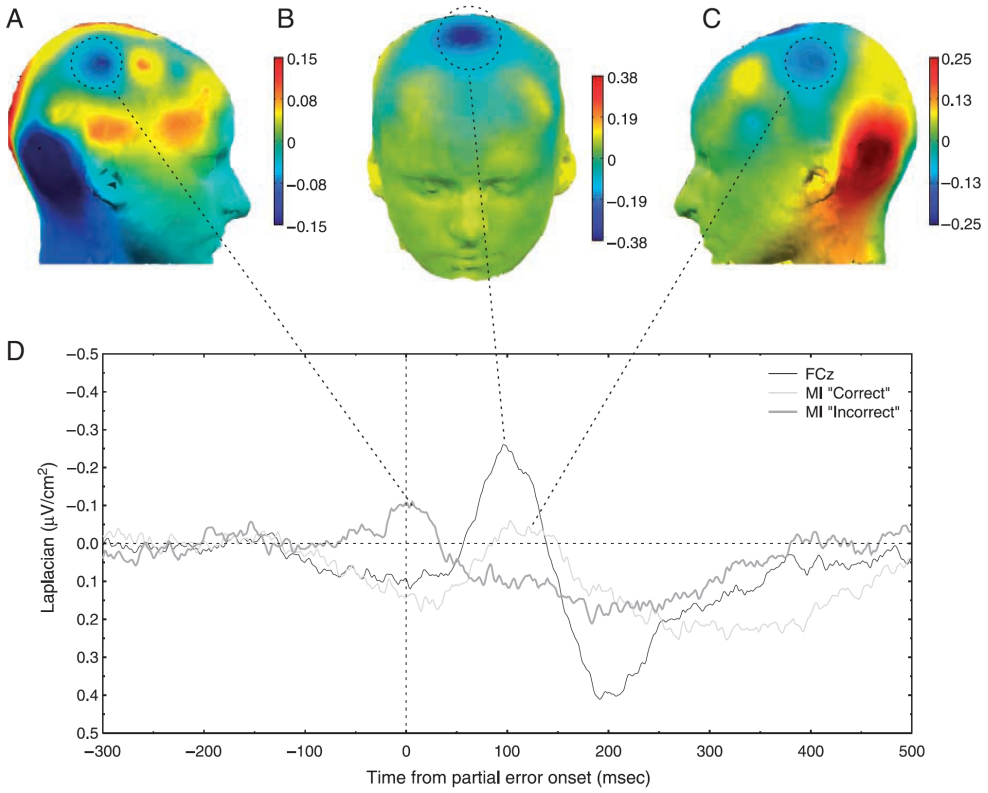

FIGURE 3.8 – **Topographies and time-courses of the activities under interest.** For sake of simplicity, the activities related to the two responses were averaged after mirroring the activities for the left response : activities recorded over the left electrodes for the were projected to their corresponding right ones, and vice-versa. Thus C3 corresponds to the primary motor cortices contralateral to the correct response, whereas C4 corresponds to the primary motor cortices contralateral to the incorrect response (*i.e.* the partial error. Except when noted, the baseline for the maps have been taken between -500 and -100 a) Laplacian (CSD) map obtained at incorrect activation time (9 ms after EMG onset). One observes a clear activity localized over C4, that is at the level of the primary motor cortex involved in the incorrect response. b) Laplacian map obtained at the peak of the N_E. The topography is clearly fronto-central, compatible with source(s) in the ACC and/or in the SMA. c) Laplacian map at the time of the correct response activation. One can observe a clear activity nicely localized over C3, that is over the primary motor cortices contralateral to the correct response. Note that, because of the positivity starting just before partial error onset (likely reflecting an inhibition, see Burle et al., 2004), the baseline was taken between -50 and 50 ms.

EMG burst is longer when the interval between the incorrect and the correct response increases (see Figure 3.5), the degree of overlap between the two EMG activities is virtually null, except maybe when the interval is very small. Thus, as long as response activation is evaluated at the EMG level (Yeung *et al.*, 2004), the incorrect and correct response activations did not overlap in any of the trials, and the conflict is null in this dataset. The apparent overlap observed on Figure 3.6 stems from the fact that the *slowest* incorrect activations occur later than the *fastest* correct ones, but not on the same trials. This exemplifies the hazards of averaging procedures, since, although we do observe "conflict" on averaged data that very nicely fit the predictions of the model, there is no "conflict" (as defined in the model ...) at all, on any of the trials, in this dataset.

One may argue, however, that even if co-activation does not occur at the EMG level, it might well be present at the central level. We thus analyzed the activity of the primary motor cortices contralateral to the incorrect and correct responses. Indeed, thanks to Laplacian estimation, it recently became possible to estimate the activation of the two primary motor cortices separately in choice RT tasks (Praamstra et Seiss, 2005; Tandonnet *et al.*, 2003; Taniguchi *et al.*, 2001; Vidal *et al.*, 2003b, see Burle *et al.*, 2004b for an overview).

The second row of Figure 3.7 presents the cortical activation of the incorrect response, *i.e.* the activity of the primary motor cortices controlateral to the partial error (left column) and the cortical activation of the correct one, *i.e.* the activity of the primary motor cortices controlateral to the correct response. The topographies of these activities, along with that of the N_E, are presented in Figure 3.8.

The signal/noise ratio of EEG being much lower than that of EMG, the results have to be interpreted with some caution. Some systematic patterns emerge nonetheless : the incorrect response activation, as measured at the primary motor cortices contralateral to the incorrect response, starts just before incorrect EMG onset (blue strip on Figure 3.7C), peaks shortly after EMG onset and then decreases back to baseline, or slightly below. It seems that the incorrect response activation is over about 30-40 ms after incorrect EMG onset. The correct response activation (Figure 3.7D) follows the Δ value and starts later as this value increases. More importantly, the activation of the correct response clearly starts after the end of the incorrect response activation, and there seems to be virtually no overlap between the incorrect and correct response activation. Thus, here again, no conflict, as defined in the model, seems to emerge at the primary motor cortices level. We shall return to this absence of "conflict" in the Discussion.

Another interesting aspect is to be noted : when comparing the dynamics of the incorrect response activation and of the N_E (see Figure 3.3A), it appears that the N_E invariably starts

around the end of the incorrect response activation. Since it starts *after* the end of the incorrect activation, the N_E cannot be responsible for the interruption of the incorrect response activation as this incorrect response activation had necessarily been detected earlier in order to be stopped. Thus, the N_E cannot reflect the detection of this incorrect response activation, invalidating a simple error-detection mechanism (see Gehring et Fencsik (1999) for similar arguments on EMG).

For the sake of comparison, we also plotted the ERP-images of the incorrect and correct response simulated activations. The third row of Figure 3.7 presents the single–trial dynamics of the incorrect (panel E) and correct response (panel F) activations obtained in the simulation. The incorrect response starts being activated just before the partial error onset, and lasts almost until the correct response. The incorrect response starts being de-activated when the correct response starts being activated. The conflict, depicted on Figure 3.3B, thus peaks just before the correct response, when the two responses are still activated and are maximally competing.

3.4 Discussion

In the last few years, the conflict–loop theory (Botvinick *et al.*, 2001, 2004, 1999; Carter *et al.*, 1998, 1999; Cohen *et al.*, 2000; Yeung *et al.*, 2004) has played a key role in cognitive control research since it proposed a unified model that aimed to account for both behavioral and neurophysiological data. The model introduced a very simple, though elegant, concept : response-conflict is defined as the degree of co-activation of the possible responses. It has been argued that monitoring conflict allows, without any "clever" cognitive system, to detect failures in ongoing processing, and to adjust subsequent behavior. The model explicitly relates conflict monitoring with ACC activity as observed with metabolic measures, and through specific EEG components. The main EEG component related to conflict is the N_E. We will first discuss the relationship between the N_E and conflict, and then discuss the very concept of conflict as a relevant notion for cognitive control.

3.4.1 N_E and conflict

The N_E has played an essential role in the development of the conflict model (Botvinick *et al.*, 2001, 2004; Yeung *et al.*, 2004). Reciprocally, the conflict model has been extremely influential in the N_E literature, since a lot of studies have used the conflict model as a general framework for interpreting their results. However, although several studies have tested the conflict interpretation of ACC activity observed in metabolic research (Brown et Braver, 2005; Egner et Hirsch, 2005a), few studies have explicitly addressed the conflict model hypothesis on the N_E, apart from the conflict

modelers themselves (Botvinick *et al.*, 2001; Yeung *et al.*, 2004, see Carbonnell et Falkenstein, 2006 for an exception). Here, we directly tested the conflict interpretation of the N_E by estimating the amount of conflict on a trial-by-trial basis by analysing partial error trials (Figure 3.1) that allow, on a single trial basis, to track the activation of incorrect and correct responses. According to the definition of conflict, we reasoned that conflict should depend on the temporal overlap between the two response activations, that we measured through the Δ value. A simulation confirmed that the amount of conflict depends on the Δ between the two response activations : the smaller the Δ between the incorrect and correct response activations, the larger the conflict. However, the present experiment shows that the N_E decreases as the Δ decreases, therefore demonstrating that the N_E evolves in a way opposite to the conflict. The mandatory conclusion that derives from the present study is that the N_E does not reflect conflict. A note concerning the model's prediction regarding metabolic signal is in order. Indeed, it is important to note that fMRI, because of its low temporal resolution, provides information of a different nature compared to EEG : the measured signal represents a *temporal integration* of brain activity. In this respect, the BOLD signal should not be compared to the peak amplitude of the conflict, but more likely to the overall conflict, that is the surface under the conflict curve (*i.e.* the integral of the conflict over time). That is actually what Botvinick *et al.* (2001) did in their first simulations that sought to compare the conflict predictions with ACC activations obtained with fMRI. Integrated conflict was measured and analyzed in the section "Alternative measure of conflict", and the results show that the integrated conflict is the same whatever Δ. Thus, interestingly, the model would predict no change in ACC BOLD response, as a function of Δ, despite the fact that conflict is clearly affected by Δ. This confirms that timing is essential for an appropriate test of the model.

The main hypotheses of the conflict model were : 1) the amount of conflict is monitored by the ACC, 2) the electrophysiological correlate of conflict monitoring is the N_E, 3) conflict triggers cognitive control which results in subsequent adjustments in behavior. The present data clearly invalidate prediction 2. Recently, prediction 3, namely that sequential effects depend on conflict, has been put into test by Burle *et al.* (2005). The results demonstrated that conflict, as assessed by incorrect response activation and reflected by the N_E, is *not sufficient* to account for sequential adjustments. Concerning prediction 1, one may argue that the ACC indeed measures conflict, but that the N_E does not reflect such a conflict monitoring. Although this considerably weakens the model, this view could save (a part of) it. This is, however, unlikely. Indeed, several source localization studies have pointed out that the N_E has a source in the ACC (Dehaene *et al.*, 1994; Van Veen et Carter, 2002), although other areas, including the Supplementary Motor Area, might

also contribute to the N_E (Dehaene *et al.*, 1994; Herrmann *et al.*, 2004; Stemmer *et al.*, 2004). Furthermore, recent co-registration of EEG and fMRI provided a strong argument in favor of the idea that the ACC is at least involved in the genesis of the N_E (Debener *et al.*, 2005). Hence, ACC activity, as assessed by fMRI, and N_E are likely to be strongly related.

A recent report, in light of other studies, further suggests that ACC does not monitor response conflict : di Pellegrino *et al.* (2007) showed that ACC is *necessary* for sequential adjustments to occur (see also Kerns *et al.* (2004)), while Burle *et al.* (2005) showed that response conflict is *not sufficient* to trigger those adjustments. Taken together, those two studies clearly dissociate ACC and response conflict monitoring.

Considering the above arguments, the most parsimonious position is to assume that, although ACC seems clearly involved in detecting the need for more cognitive control, it does not do so through conflict monitoring (Egner et Hirsch, 2005a; Nakamura *et al.*, 2005).

3.4.2 Response co-activation, conflict and behavioral interference

Besides the interpretation of the N_E and ACC activity in terms of conflict, the present data also question the very notion of response conflict – or response competition – as a universal explanation for both behavioral interference and ACC activity. Indeed, the EMG data clearly indicate that there was no co-activation of the responses at such a peripheral level, and the same conclusion seems to hold also at the level of primary motor cortex. Even for trials in which the incorrect response was undoubtedly activated, the correct and incorrect responses are never activated at the same time, casting some doubt on the general idea that the responses are competing. Before we go further in this direction, a comment is in order : the fact that there was no co-activation in the present dataset does not imply that co-activation is never obtained. As a matter of fact, Carbonnell et Falkenstein (2006) did observe overlap between response force traces on a trial–by–trial basis. Thus the presence of overlap between response activations might well depend on the specific parameters of the task. In any cases, the important point is that, even without co-activation, the present dataset clearly show an interference effect on RT. Thus, if co-activated responses compete, inducing an interference, the present data show that *response*–competition is not necessary for interference to occur. Co-activation seem also lacking at the primary motor cortices level. Note that, although they are not the only areas involved in actual response activation, there is general agreement that MI plays an essential role in the implementation of the motor command. Thus, if behavioral interference is due to a competition between mutually exclusive representations, such a competition does not

occur at the motor execution level (Burle *et al.*, 2002b; Rösler et Finger, 1993) but more likely upstream in the information processing chain, contrary to what is often assumed (Coles *et al.*, 1985; Gratton *et al.*, 1988, see however Valle-Inclán et Redondo, 1998). This may sound at odds with a rather large amount of data, empirical and theoretical, suggesting that response-competition is at the core of interference effects. However, it is to be noted that (almost) all arguments for motor co-activation come from EEG data, employing averaging procedures. Importantly, our averaged data also seem, at first sight, in agreement with motor co-activation (see Figure 3.6). However, as described above, the apparent co-activation stems from an artifact introduced by averaging and when one looks at the same data with methods that avoid the production of such an artifact, the observed pattern leads to the opposite conclusion. One may thus wonder whether similar artifacts are present in the literature (see Meyer *et al.* (1988) for similar concerns) and the arguments for co-activation of motor components may need to be re-evaluated.

Note, however, that the absence of co-activation of responses does not preclude the possibility of co-activation of mutually exclusive representations upstream from the primary motor cortices. Indeed, competition might well occur at more abstract (or central) levels. In this case, this would mean that interference does not occur at the motor level (Burle *et al.*, 2002b; Rösler et Finger, 1993; Valle-Inclán et Redondo, 1998), but at other stages of information processing. Thus, the present results might remain compatible with "competition" views, but push the location of such a competition upstream in the information processing chain.

3.4.3 Relations to other models of ACC/N_E function

The present data clearly invalidate the interpretation of the N_E in terms of conflict, defined as the co-activation of two responses. Some alternative models of ACC function and of the N_E have been proposed recently. We shall now discuss the implication of the present data for these models.

The Reinforcement–Learning Theory of the N_E

Holroyd and colleagues Holroyd et Coles (2002); Holroyd *et al.* (2005) proposed an alternative formal model of the N_E and ACC function [5]. This model is based on reinforcement–learning theory Sutton et Barto (1998) that implements the so-called *temporal difference error*. It is beyond our

5. Brown et Braver (2005) proposed a modified version of Holroyd et Coles (2002)'s model : the so-called "Error–likelihood" model. It aims mainly at accounting for metabolic data, and a recent test of the model for electrophysiological data invalidate some of its main predictions Nieuwenhuis *et al.* (2007). We will thus not further discuss this model here.

scope to describe the model in detail. We will briefly present the features that are relevant for evaluating the impact of the present results for this model. The most recent version of the model Holroyd *et al.* (2005) for (a modified version of) the Eriksen task is made of two components : a task module and a monitor module. The task module implements the operations necessary to solve the task. It is composed of three layers : an input layer (coding for the letters presented at each position – *i.e.* "H" on left position, or "S" on the center position etc...), a category layer (representing a decision concerning the nature of the central – *i.e.* the target – letter) and a response layer (representing the two possible responses) [6]. The category and the responses layers continuously send their level of activity to the monitor module. The monitor module is also composed of several layers, but we will present only the relevant ones. One set of units, so called *conjunction units* receive activation from the category and response units and code for the conjunction of the two (*i.e.* the HL unit receives activation from the stimulus unit H and the response unit L. Its activation thus indicates that the target H and the response L have been activated). There are thus four conjunction units (2 targets $\times$ 2 responses), and each of these units is associated with a *value*, that can be positive if the conjunction corresponds to a correct response, or negative in the opposite case. For example, if the instruction is to give a left response when the target is "H", the value of HL will be positive, whereas the value of HR ("H" target and right response) will be negative. A *Temporal difference* unit (TD) receives inputs from the conjunction units, integrates them and issues a temporal difference signal, that will be an error signal in the case of incorrect response. More formally, since no more than one unit can be active at any time (Holroyd *et al.*, 2005, p. 179), the activation a^t_{TD} of the TD at time t amounts to :

$$a^t_{TD} = S_t \times V_s \tag{3.4}$$

where S_t is the present state of the system (the level of activity of the conjunction unit, if any) and V_s is the value of this state (Note that this corresponds to basic definition of conditioning learning processes, see Sutton et Barto (1990)). The temporal difference signal at time t, whose amplitude corresponds to the N_E, is defined as :

$$\delta^t = a^t_{TD} - a^{t-1}_{TD} \tag{3.5}$$

that is the difference between two successive time steps (represented as cycles in the model).

Can this model account for the present data ? Although the simulations reported by Holroyd *et al.* (2005) were only concerned with overt errors, one can easily assume that an error signal could

6. An attentional layer is also present in the task module, biasing stimulus and response processing. However, since the impact of the attentional layer is not relevant here, we will not discuss it further

be generated by partial errors [7]. Thus in principle, partial error could certainly induce an N_E in this model. Furthermore, according to the way the error signal is generated, it is likely that the predicted N_E would be much more time-locked to the partial error onset than would the conflict (cf. Figure 3.3B) and, hence, more similar to the experimental N_E (cf. Figure 3.3A), although some simulations are certainly needed to better confirm this hypothesis. However, without significant modification, the model does not seem able to account for the relationship between N_E amplitude and Δ values. Indeed, as clearly stated by (Holroyd *et al.*, 2005, p. 178) "[...] the first unit of each pair [of task state units] to be activated remains active until the end of the trial. Critically, if the task module generates a second response following an error (an *error correction*), the response detection unit activated by the initial response remains active, and the response detection unit associated with the second response remains inactive. [...]". Thus, even if the task module could correct an error, the monitor module would be blind to such a correction, and hence the error signal could not be sensitive to the timing of such a correction.

If we relax this constraint, one may wonder whether a modified version of the reinforcement learning hypothesis could account for the data. Given that the value of a given state is constant during a trial (even if it can vary during learning), it appears from eq. 3.4 that the evolution of the N_E will only depend on the time course of S_t. If one accepts that, after initial activation of an incorrect conjunction unit (triggering an error signal, represented as a negative TD signal, see Holroyd *et al.* (2005)), a correct conjunction unit can later be activated, the activation of this correct unit will trigger a positive TD signal that will counteract the negative one (*i.e.* interrupt the error signal). Interestingly, in this case, there will be a monotonic relationship between the end of the error signal and the correction : the later the correction, the longer the duration, and probably the greater the activation, of the error signal. This would correspond to the N_E results (Figure 3.3C). Obviously, such a possibility needs to be implemented and tested in future simulations.

3.4.4 Online control of control ?

Besides the invalidation of the conflict account, the present results also provide insights that may help in deciphering the functional significance of the N_E.

In the present data set, the latency and dynamics of the N_E onset are independent of the interval between incorrect and correct response activations, suggesting that the N_E induced by the partial error initially develops in the same way whatever the timing of the correction. The N_E,

7. In a way similar to that conducted for the conflict model.

however, lasts longer and reaches a higher amplitude when this interval increases (Figure 3.3 A and C). After this initial development, the N_E seems interrupted. This interruption correlates with the timing of the correct response activation : the later the correction, the later the interruption, in agreement with data obtained by Fiehler *et al.* (2005) who observed that the N_E on overt errors peaks later when the correction of the error is slow.

The N_E initial development is similar whatever the timing of the correction, suggesting that the N_E is *a priori* the same, and hence that the observed differences occur later in time. This indicates that the N_E can be modulated "online", that is during the course of a trial. Furthermore, the N_E interruption being directly linked to the correction, it seems that the N_E is suppressed once the remediation process has started. This suggests that the ACC activity is used as an "alarm signal", which lasts until remediation processes take place, making such an alarm signal useless. In this case, this would indicate that the need for control is also monitored and adjusted online, during the course of a trial. In the above discussion of the reinforcement–learning model of the N_E, we have seen some possible directions on how this model could implement such an idea. Whatever the exact nature of this signal, since it is highly dynamic and flexible, this opens new perspectives, and adds constraints on possible modeling of the evaluation processes.

3.5 APPENDIX A

Single trial dynamics

In order for all the participants to have the same weight on all the "trials" of the ERP–Images, we have computed the ERP–images for each participant separately, and then averaged the ERP–Images. ERP–Images are in fact matrices of size `number_of_points` × `number_of_trials`. The value of `number_of_trials`, however, is not constant across subjects, since it depends on the number of partial errors. Thus the matrices for the various subjects had not exactly the same size, precluding direct averaging of the matrices and hence of the ERP-Images. In EEGLAB, the `number_of_trials` value in the matrix can be reduced by applying an inter-trial smooth Jung *et al.* (2001). One can thus theoretically reduced the dimensions of all the matrices of all the subjects to the same value. This, however, necessitates large smoothing values for the subjects presenting a lot of trials, given the large differences in number of trials (see table 3.1). We therefore choose a balanced option, by both decreasing the dimension of the matrices containing the largest number of trials by applying an appropriate smooth implemented in EEGLAB, and by increasing the size of

TABLE 3.1 – Summary of the number of partial errors and of the smoothing/interpolation procedure applied to the individua data. The final number of "trials" (*i.e.* rows in the matrix) was set to 216, since i) two participants had this number of trials, and ii) it seemed a good compromise between smoothing (reducing dimension) and interpolation (increasing dimension).

Subject N°	Partial errors	Smooth	Interpolation	Final
1	216	-	-	216
2	92	-	124	216
3	236	20	-	216
4	146	-	70	216
5	279	63	-	216
6	268	52	-	216
7	173	-	43	216
8	277	61	-	216
9	267	51	-	216
10	216	-	-	216

the matrices presenting a low number of trials, by applying an interpolation of the image accross the trials. Note that the interpolation does not change anything to the image but its size. The information conveyed by the ERP-Image is thus kept constant, as exemplified in Fig. 3.9. The smoothing/interpolation procedure applied to each individual participant is presented on table 3.1.

3.6 APPENDIX B

Chronometry of partial errors

In the experimental data, the latency of the partial error onset decreased from class 1 (Δ values from 101 ms to 150 ms) to class 4 (from 251 to 300 ms), $F(3, 27) = 21.2; p < .001$, linear component, $F(1, 9) = 34.05; p < .001$. Symetrically, the latency of the correct response increased, $F(3, 27) = 59.81; p < .001$, linear component : $F(1, 9) = 86.13; p < .001$. Thus the increase in the Δ values is due to both earlier partial errors and later correct responses (see Table 3.3). A similar pattern was obtained in the simulation : The latency of the partial error onset decreased from class 1 (from 2 to 4 cycles) to class 4 (from 11 to 13 cycles), $F(3, 27) = 77.97; p < .001$, linear

TABLE 3.2 – Summary of the number of partial errors and of the smoothing/interpolation procedure applied to the simulation. The final number of "trials" (*i.e.* rows in the matrix) was set to 67.

Simulation N°	Partial errors	Smooth	Interpolation	Final
1	68	1	-	67
2	67	-	-	67
3	63	-	4	67
4	57	-	10	67
5	71	4	-	67
6	74	7	-	67
7	57	-	10	67
8	49	-	18	67
9	85	18	-	67
10	67	-	-	67

component, $F(1,9) = 188.12; p < .001$. Symetrically, the latency of the correct response increased, $F(3,27) = 70.87; p < .001$, linear component, $F(1,9) = 169.27; p < .001$ (see Table 3.4). Thus, as for the experimental data, the increase in the Δ values is due to both earlier partial errors and later correct responses. More importantly, the partial error recorded experimentally and simulated behave in the same way, making the two highly comparable.

TABLE 3.3 – Mean chronometric indices (in ms) obtained in the experiment for the partial error trials.

	Partial error onset	Response Time	Δ value
class 1	277	410	133
class 2	260	440	180
class 3	246	481	235
class 4	237	505	267

TABLE 3.4 – Mean chronometric indices obtained in the simulation for the partial error trials. All the values are given in number of cycles.

	Partial error onset	Response Time	Δ value
class 1	6.21	9.79	3.58
class 2	4.42	10.61	6.18
class 3	2.94	12.12	9.18
class 4	2.14	14.13	11.99

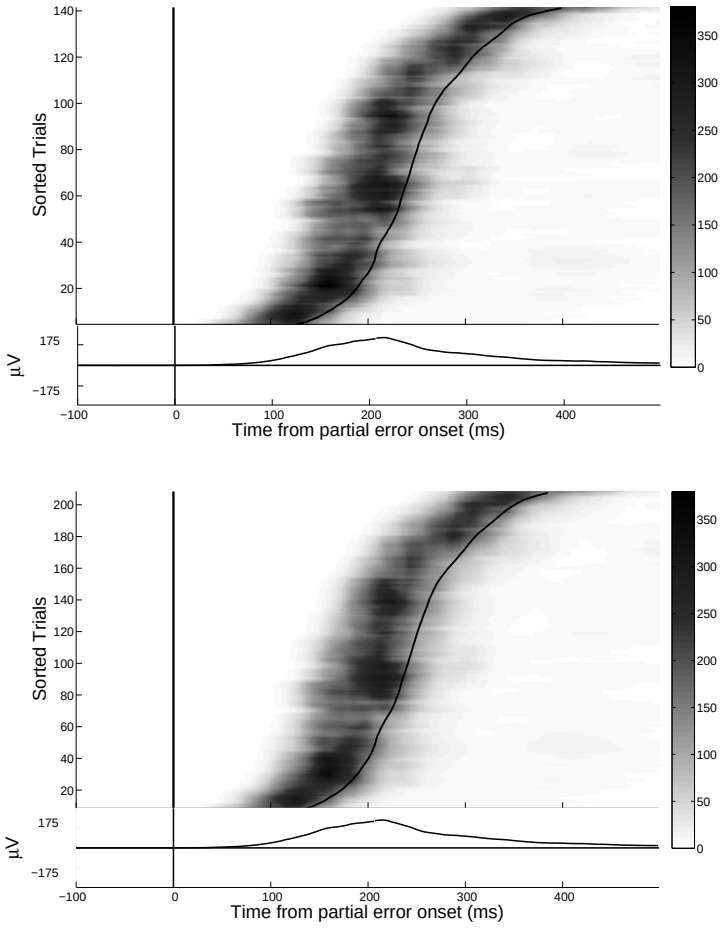

FIGURE 3.9 – **Impact of interpolation on the time-course of activity of interest :** The top figure represents the ERP image of EMG activity for subject N° 4, before interpolation (number of trials = 146), and the bottom figure represents the same data after interpolation (number of "trials" = 216). As one can see, the interpolation did not introduce any distortions nor remove any obvious proporties of the signal. Colorbar are in μV.